Journal of Energy Research and Reviews

7(3): 27-45, 2021; Article no.JENRR.67379
ISSN: 2581-8368

Approaching an Efficient and Feasible Carnot Engine by Carnot Cycle Analysis

Ramon Ferreiro Garcia[1*]

[1]Ind. Eng. Department, University of A Coruna, Spain.

Author's contribution

The sole author designed, analyzed, interpreted and prepared the manuscript.

Article Information

DOI: 10.9734/JENRR/2021/v7i330193
Editor(s):
(1) Dr. Hasan Aydogan, Selcuk University, Turkey.
Reviewers:
(1) Vedran Mrzljak, University of Rijeka, Croatia.
(2) Ti-Wei Xue, Tsinghua University, China.
Complete Peer review History: http://www.sdiarticle4.com/review-history/67379

Original Research Article

Received 06 February 2021
Accepted 12 April 2021
Published 19 April 2021

ABSTRACT

Based on the knowledge exhibited in the literature on the Carnot cycle, a preliminary study is carried out on Carnot machines capable of implementing the Carnot cycle at high thermal efficiency. Therefore, two engine structures are proposed: (i) reciprocating single and double-acting cylinder-based thermal engines implemented under a closed processes-based Carnot thermal cycle characterised by a mechanical structure internally coupled, and (ii) similar engines characterised by a mechanical structure internally decoupled.

In order to perform the cycle analysis, however, observational (experimental) evidence confirms on a daily basis the fact that there are two performance criteria: conventional (output net work/input heat) thermal efficiency and output/input energetic-based first law efficiency. Based on such premises, this study investigates both coupled and decoupled Carnot engine structures.

The results confirm that an important fraction of heat can be converted into useful work by configuring a decoupled structure of the Carnot engine.

Indicative results support the use of internally decoupled thermal machines, especially when the heat source has a low or medium temperature. Even at high temperatures, such machines are advantageous in terms of energy efficiency. Furthermore, avoiding internal coupling allows for power regulation without disturbing interactions due to variations in load, thus enabling robust control.

**Corresponding author: E-mail: ramon.ferreiro@udc.es;*

Keywords: Carnot engine; carnot efficiency; carnot factor; energetic efficiency; internally decoupled machines.

ABBREVIATIONS

Symbol	Nomenclature/units
n	polytropic exponent
γ	adiabatic exponent
C_V	specific heat at const. vol. (kJ/kg.K)
η_{th}	thermal efficiency (%)
η_E	energetic efficiency, Energ.eff (%)
η_c	Carnot efficiency, Carnot factor (%)
h	specific enthalpy (kJ/kg.K)
p	pressure (bar)
q	specific heat magnitude (kJ/kg)
q_i	specific heat in (kJ/kg)
q_o	specific heat out (kJ/kg)
R	ideal gas constant [*Cp*-*Cv*] (kJ/kg.K)
s	specific entropy (kJ/kg.K)
T	temperature (K)
T_H	top temperature (cycle) (K)
T_L	bottoming temperature (cycle) (K)
u	specific internal energy (kJ/kg)
v	specific volume (m^3/kg)
V	volume (m^3)
w	specific work (kJ/kg)
w_i	specific work in (kJ/kg)
w_o	specific work out (kJ/kg)
w_n	net specific work (kJ/kg)

Acronyms	Meanings
CF	Carnot factor, Carnot efficiency
cpb	closed process-based
FCF	forced convection fan
HE	irreversible heat engine
HEr	reversible heat engine
Hex	heat exchanger
HTF	heating transfer fluid
sp	thermal state point
TWF	thermal working fluid
TC	temperature controller
TT	temperature transmitter

1. INTRODUCTION

1.1 Introduction and Background

In 1824, Carnot proposed an ideal reversible thermal cycle operating on reversibility conditions [1]. He proved that there exists an upper limit of the efficiency of this ideal reversible thermal cycle, and, according to him, *this limit is applicable to any real thermal cycle*. However, Carnot's theorem limits the thermal efficiency of the Carnot cycle, including Carnot-like cycles such as ideal Stirling and ideal Ericsson cycles.

The Carnot cycle is designed to operate exclusively as a reversible ideal Carnot engine. Carnot's principle states that "*no heat engine (H**E**) can be more efficient than a reversible one (H**er**) operating between the same temperatures.*" This relevant statement asseverates that *any irreversible engine is less efficient than the same reversible engine*. Nevertheless, this statement does not make any reference to the impossibility of converting heat to mechanical work under a limited or restricted conversion ratio to any given value. Thus, it does not refer to the impossibility of designing ideal thermal machines that are more efficient than the Carnot engine.

Thus, since the Carnot engine operates exclusively under a Carnot cycle, it is not a real thermal engine requiring that all cycle processes are reversible. As a consequence, no type of real machine or thermal working fluid is considered. However, it is used as a benchmark that is useful when approaching the thermal efficiency or performance of conventional thermal engines, which are designed to be as close as possible to the Carnot engine.

In terms of Carnot's theorem's usefulness, how can a concept that cannot exhibit real existence be compared with a real entity? It can be done only if Carnot efficiency is considered as an unattainable goal.

Accordingly, the non-existent concepts of the Carnot cycle and its efficiency are useful as unattainable goals against which existing technologies can be compared. This does not mean that a technological paradigm shift cannot exceed a goal set by the Carnot factor.

However, the concept of Carnot efficiency explains that even under ideal conditions (without dissipation), there are physical reasons for avoiding converting all the energies absorbed by the cycle in mechanical work. Therefore, it is worth trying to design a real thermal engine capable of coming as close to the Carnot factor as possible.

When trying to approach a real and efficient Carnot engine in the first place, it must be considered that the ideal Carnot cycle operates without a thermal working fluid. It is known that the characteristics of a thermal working fluid are one of the conversion factors that heavily influence the efficiency of the thermal cycle. Another important factor is the heat-work conversion ratio (w/q) of the thermal process carried out in any thermal cycle. The conversion ratio depends on the characteristics of the working fluids and the path function. Another crucial factor is the structural conception of the thermal engine. Heat transfer facilities (internal and external irreversibilities) and external environment conditions also contribute to the efficiency of the cycle. The limits of the thermal efficiency of real thermal cycles depend on many factors besides Carnot constraints. The conversion of total heat to work requires that for every conversion process in a thermal cycle satisfies the condition that (w/q) = 1.

The advances made in the Carnot cycle over the last two decades concern general aspects rather than the approximation of a real machine using the Carnot cycle. F. Moukalled [2] used endoreversible thermodynamics to study the performance of Carnot engines with heat leaks, showing that the efficiency at maximum power output is significantly affected by the rate of heat leak. M. Bojić [3] found that the production of heat and power is maximised when the products of the size and heat transfer coefficients on the hot and cold sides of the heat exchangers of the Carnot engine are equal. Also, the ratio of the lower and higher temperatures of the Carnot engine should present optimal values.

Stanislaw Sieniutycz [4] analysed an irreversible extension of the Carnot problem of maximum mechanical work delivered from a system that involves two fluids of different temperatures. Ali Kodal et al. [5] reported finite time thermodynamic optimisation based on the maximum power density criterion for an irreversible Carnot heat engine.

Francesco di Liberto [6] proposed a stepwise Carnot cycle performed by means of N small weights (called dw's), which were first added and then removed from the piston of a vessel containing the gas. The results show that the work performed by the gas can increase the potential energy of the dw's. N. Sánchez Salas et al. [7] presented the results of efficiency and power output for irreversible Carnot-like heat engines with nonlinear inverse, Dulong-Petit, and Stefan-Boltzmann heat transfer laws when optimised with a recent criterion.

S.K. Tyagi et al. [8] performed a parametric study of irreversible Stirling and Ericsson cryogenic refrigerator cycles as a paradigm of Carnot cycle applications. Lingen Chen et al. [9] approached an optimal configuration and the fundamental optimal relationship between the cycle's power output and efficiency, discussing some special examples. The authors claim that some theoretical guidance for the design of practical engines was achieved.

M. Feidt et al. [10] proposed a model for studying and optimising thermal machines with two heat reservoirs. The authors claim that once it is proven that one of the possible objective functions is fixed (as a parameter with imposed value), the optima of the other three always correspond to each other for the corresponding stationary state system, with a given optimum heat conductance allocation for one degree of freedom. Jonathan M. Cullen et al. [11] conducted a study aimed at calculating absolute potential to reduce energy demand by improving efficiency (they did this by finding the efficiency limits for individual conversion devices).

Hamza Semmari et al. [12], showed that a thermodynamic engine cycle can be implemented by exploiting the temperature difference that exists between warm surface seawater and cold deep seawater. The engine is based on a new Carnot-based cycle for OTEC applications (called the CAPILI cycle). In this new engine cycle, work is produced by the movement of an inert liquid through a hydraulic turbine. In the work of Bing Zhou et al. [13], the concepts of entransy and entropy are applied to analyses of the irreversible Carnot engines based on finite time thermodynamics.

Blaise M. et al. [14], studied a Carnot type engine with a phase that changed during heating and cooling that was modelled with its thermal contact with the heat source. Martínez I. et al. [15] present an exhaustive study of the

energetics of the engine. Their analysis of the fluctuations of finite-time efficiency shows that the Carnot bound can be surpassed for a small number of non-equilibrium cycles.

Michel Feidt [16] presented an extension and generalisation of the model proposed by Carnot. Mathilde Blaise et al. [17] attempted to define an upper bound for waste heat to power conversion that depends on the waste heat temperature and its available mass flow rate, the working fluid used, and the exchangers' size. Based on this, the researchers attempted to model and optimise a Carnot-type engine with a changing phase working fluid.

Fontaine K, et al. [18] present a method for evaluating heat exchangers for OTECs based on finite-time thermodynamics. In their method, the maximum net power output for different heat exchangers (which use both heat transfer performance and pressure drop) was assessed and compared to improve performance. Michel Feidt et al. [19] aimed to enrich the model and further the debate by emphasising the fundamental role of the heat transfer entropy and the production of entropy when accounting for the external or internal irreversibilities of the converter. They emphasised the main consequences of the approach and obtained new limits of efficiency at maximum energy or power output.

The remainder of the current work is organised as follows. Section 2 describes the analysis of potential viable Carnot cycle structures. Section 3 describes the implementation of coupled and decoupled Carnot machines. Section 4 explains the case study. Section 5 discusses the results of the studied cases. Section 6 presents the conclusions derived from the analysis.

2. VIABLE THERMAL ENGINE STRUCTURES CAPABLE OF SUPPORTING A CARNOT CYCLE

All thermal cycles are associated with a specific thermo-mechanical structure. Generally, in terms of internal mechanical couplings, there are two groups of thermal engine structures: internally decoupled and internally coupled structures. Double and single-acting reciprocating thermal engines are inherently internally coupled. However, it is possible to construct decoupled reciprocating engines with modular structures.

Fig. 1 depicts several engine structures to illustrate the concept of internal and external mechanical couplings. The difference between coupling and decoupling structures is an essential and relevant characteristic that determines the efficiency of the thermal engine.

2.1 Modelling and Analysis of the Thermo-structural Characteristics of Closed Processes-based Thermal Engines

2.1.1 Decoupled thermal engine structure

Internally decoupled thermal engine cycles for closed processes are modelled according to Fig. 1 (a) and (b). All types of losses neglected from the heat-work interactions considered in this analysis are assumed to be based on the 1st law.

Input energy

$$E_i = q_i + w_i \tag{1}$$

Output energy

$$E_o = q_o + w_o \tag{2}$$

$$E_i - E_o = (q_i + w_i) - (q_o + w_o) = 0 \tag{3}$$

From (4), it follows that

$$q_i + w_i = q_o + w_o, \text{ and } q_i - q_o = w_o - w_i \tag{4}$$

The above equation (energy balance) defines the 1st law for a thermal cycle, which asserts that "the net input energy equals the net output energy."

The net output of useful work w_u is defined as the difference between the output and input mechanical work such that

$$q_i - q_o = w_o - w_i = w_n \tag{5}$$

The thermal efficiency η_{th} is defined as the ratio of the output useful work to the input heat. Thus, the thermal efficiency is

$$\eta_{th} = \frac{(q_i - q_o)}{q_i} = \frac{w_n}{q_i} = \frac{(w_o - w_i)}{q_i} \tag{6}$$

The energetic efficiency η_E is

$$\eta_E = \frac{(E_o - q_o)}{E_i} = \frac{w_o}{q_i + w_i} \tag{7}$$

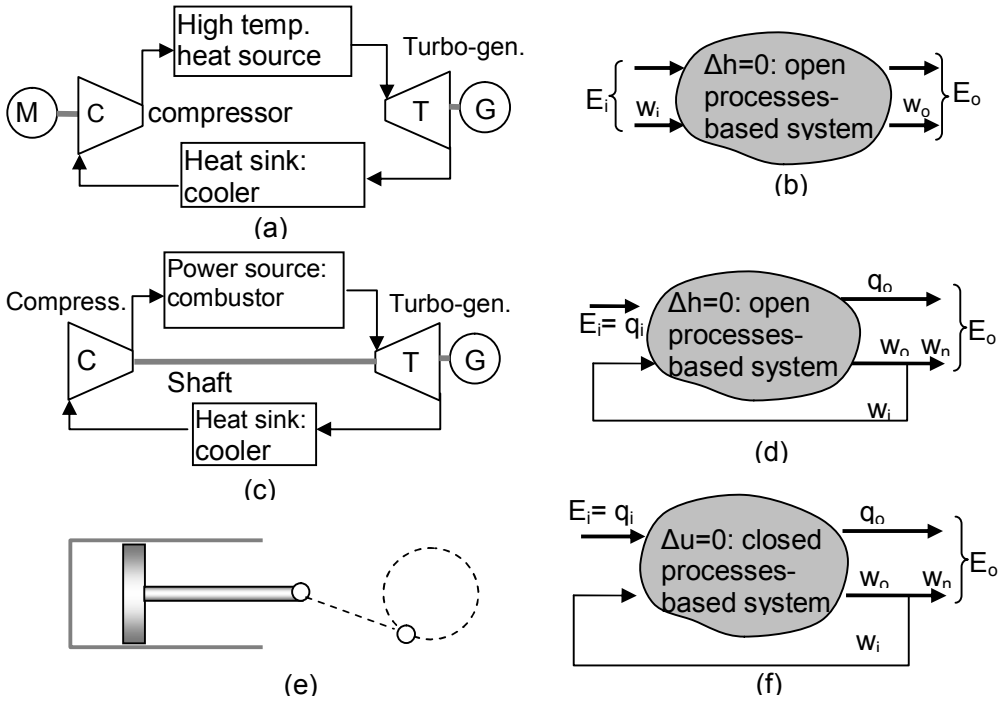

Fig. 1. Engine structures: (a) and (b) depicts the OPB Brayton internally *decoupled* thermal engine, (c) and (d) depicts the OPB Brayton internally *coupled* Brayton thermal engine, and (e) and (f) depicts a single-acting reciprocating internally *coupled* thermal engine (Stirling, Diesel, Otto structure types).

From Eqs. (6) and (7), it follows that for internally ***decoupled*** thermal engine cycles, the thermal and energetic efficiencies are different from each other.

2.1.2 Coupled thermal engine structure

The internally ***coupled*** thermal engine cycles for closed processes are modelled according to Fig.1 (b)

Input energy

$$E_i = q_i \tag{8}$$

Output energy

$$w_n = w_{o\exp} - w_{icomp} \tag{9}$$

$$E_o = q_o + w_n = q_o + w_o - w_i \tag{10}$$

From (10), it follows that

$$w_n = E_o - q_o$$

Also, from 9 and 10,

$$E_i - E_o = (q_i) - (q_o + w_n) = 0 \tag{11}$$

From (11), it follows that

$$q_i + w_i = q_o + w_o, \text{ and } q_i - q_o = w_o - w_i = w_n \tag{12}$$

The above equation (energy balance) defines the 1st law for a thermal cycle, which asserts that "the net input energy equals the net output energy."

The net output useful work w_n is defined as the difference between the output and input mechanical works such that

$$q_i - q_o = w_o - w_i = w_n \tag{13}$$

Thermal efficiency η_{th} is defined as the ratio of the output useful work to the input heat. Thus, thermal efficiency is

$$\eta_{th} = \frac{(q_i - q_o)}{q_i} = \frac{w_n}{q_i} = \frac{(w_o - w_i)}{q_i} \quad (14)$$

The energetic efficiency η_E is

$$\eta_E = \frac{(E_o - q_o)}{E_i} = \frac{w_n}{q_i} = \frac{w_o - w_i}{q_i} \quad (15)$$

From (14) and (15), it follows that

$$\eta_{th} = \eta_E = \frac{w_n}{q_i} \quad (16)$$

From (14) and (15), it follows that for internally ***coupled*** thermal engine cycles, the thermal and energetic efficiencies ***are equal***.

Table 1 shows the behaviour of thermal and energetic efficiencies as a function of mechanical coupling structures. The results are achieved through the analysis carried out by Eqs. (1)-(15). Thus, the findings depicted in Table 1 lead to the following conclusions.

Conclusion 1: The energetic and thermal efficiencies of an internally coupled thermal engine are equal.

Conclusion 2: The energetic efficiencies of two thermal engines (internally decoupled and coupled) are different from each other**.**

For the case of internally ***coupled*** thermal engine cycles, the energetic and thermal efficiencies are different. Such an apparent controversy must be solved by the following analysis.

2.2 Solving the Apparent Controversy Due to the Differences between Thermal and Energetic Efficiencies in the Case of Internally Decoupled Engine Structures

The synthesis of the performance of an internally decoupled cycle is shown in Fig. 2 from information provided by Eqs. (6) and (7), where there is a flagrant difference between both performance definitions. Therefore, the strategy to resolve this controversy consists of the following reasoning. From Eqs. (4) and (6), it follows that

$$\eta_{th} = \frac{(q_i - q_o)}{q_i} = \frac{(w_o - w_i)}{q_i} = \frac{(w_o - w_i)}{q_o + (w_o - w_i)} = \frac{a}{q_o + a} \quad (17)$$

From Eqs. (13) and (14), it follows that

$$\eta_E = \frac{(E_o - q_o)}{E_i} = \frac{w_o}{q_i + w_i} = \frac{w_o}{q_o + w_o} = \frac{b}{q_o + b} \quad (18)$$

In Eq. (17), it is assumed that $a = w_o - w_i$; in Eq. (18), $b = w_o$.

Assuming that the thermal and energetic efficiencies for internally decoupled machine structures are different from each other, the objective is to determine which of the two efficiency parameters is greater. The starting conditions for this purpose are established as follows.

$$w_o > w_i > 0;\ w_i > 0 \rightarrow (w_o - w_i) < w_o \quad (19)$$

This is the case of a Rankine cycle where the output turbine work is greater than the feed pump work—or a Brayton cycle where the output turbine work is greater than the compressor work under steady-state conditions.

$$\text{Thus, } a < b \rightarrow \frac{a}{q_o + a} < \frac{b}{q_o + b} \quad (20)$$

Therefore,

$$\text{IF } 0 < (w_o - w_i) < w_o \text{ THEN } \frac{(w_o - w_i)}{q_o + (w_o - w_i)} < \frac{w_o}{q_o + w_o} \quad (21)$$

which means that

$$\text{IF } 0 < (w_o - w_i) < w_o \text{ THEN } \eta_{th} < \eta_E \quad (22)$$

Thus, the controversy has been resolved consistently according to Eqs. (20)-(22).

A very different case is that of a heat pump, where the power of the pump or compressor exceeds that of the expander or turbine.

Theorem 1: *Energetic efficiency is greater than thermal efficiency for any thermal engine with an internally decoupled structure.*

Table 1. The behaviour of thermal and energetic efficiencies as a function of internally mechanical structures (IMS): Coupled or decoupled

IMS	Thermal efficiencies	Energetic efficiencies	comparison
Internally coupled	$\eta_{th} = \frac{(q_i - q_o)}{q_i} = \frac{(w_o - w_i)}{q_i}$	$\eta_E = \frac{(E_o - q_o)}{E_i} = \frac{w_o - w_i}{q_i}$	$\eta_{th} = \eta_E$
Internally decoupled	$\eta_{th} = \frac{(q_i - q_o)}{q_i} = \frac{(w_o - w_i)}{q_i}$	$\eta_E = \frac{(E_o - q_o)}{E_i} = \frac{w_o}{q_i + w_i}$	$\eta_{th} \neq \eta_E$

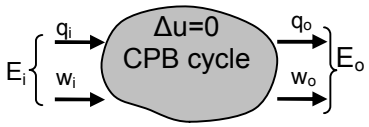

(a)

$$CPB\ \ cycle\ performance: decupled \begin{cases} \eta_{th} = \frac{(q_i - q_o)}{q_i} = \frac{(w_o - w_i)}{q_i} \\ \eta_E = \frac{(E_o - q_o)}{E_i} = \frac{w_o}{q_i + w_i} \end{cases}$$

(b)

Fig. 2. Internally *decoupled* CPB thermal engine cycle structure

The proof of the theorem has been carried out analytically through Eqs. (20)-(22).

The value of the Carnot factor is identical to the thermal efficiency of the Carnot cycle. Thus, a corollary that connects the energy efficiency of the Carnot cycle to the Carnot factor is stated as follows.

Corollary 1: *The energetic efficiency of a Carnot engine is greater than the Carnot efficiency.*

This conclusion prompts the search for internally decoupled heat engine structures on the basis that the energy efficiency is higher than the thermal efficiency. This, in turn, highlights the fact that the efficiency of an internally decoupled Carnot engine can exceed that of the Carnot factor.

3. CARNOT CYCLE

Assuming that the Carnot cycle is sufficiently mature, this introduction is intended to put into context the basic requirements for the structural design of an efficient and viable Carnot machine. Some thermal cycles designed to operate between two temperature levels (T_H and T_L) are characterised by the ability to regenerate a fraction of their own residual heat.

There are two conventional thermal cycles (characterised by doing work by adding heat or rejecting heat) that obey these mentioned characteristics: the Stirling cycle and the Ericsson cycle. However, the real objective of interest is to design a thermal machine capable not only of operating between two temperatures (high and low) but also of efficiently carrying out the processes of the Carnot cycle in an irreversible way because there is no physical possibility of escaping from the inherent irreversibilities.

3.1 Implementation of Feasible Carnot-like Engines Using a Single-acting Reciprocating Machine

Assuming that the modelling of the Carnot cycle is well-known, it is considered that it does not need any explanation so that it s exhibited as a reminder and put into context. Thus, Fig. 3 depicts the Carnot cycle in T-s and p-V diagrams. Also shown are the heats and the input and output works of the Carnot engine that are associated with the Carnot cycle [20], (Chapter 2).

The Carnot heat engine cycle depicted in Fig. 3 (a) (for the T-s diagram) and Fig. 3 (b) (for the p-V diagram), is implemented using the four reversible closed processes for an ideal single-acting reciprocating engine depicted in Fig. 4 (a)-(c). Thus, a complete cycle is composed of two strokes: the compression stroke and the expansion stroke, which are summarised as follows:
Upward stroke: Compression, Fig. 3 (a) and (b):

4-1 isothermal compression with heat extraction at T_L
1-2 adiabatic (isentropic) compression.

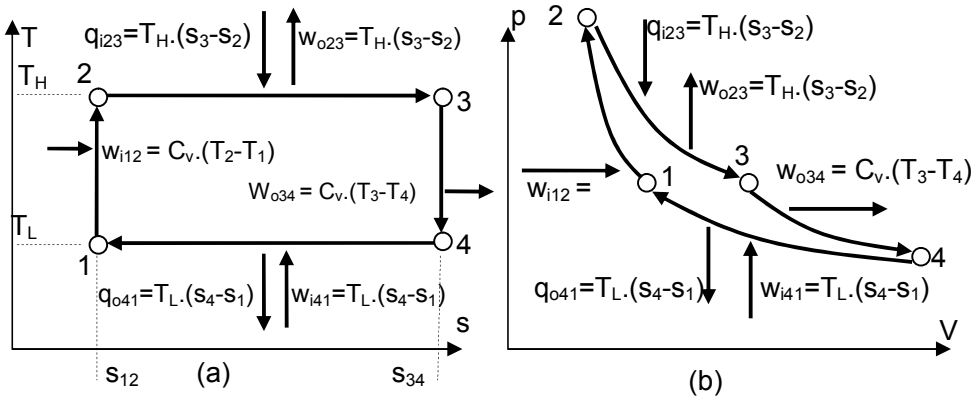

Fig. 3. The reversible Carnot cycle: (a) T-s diagram and (b) p-V diagram

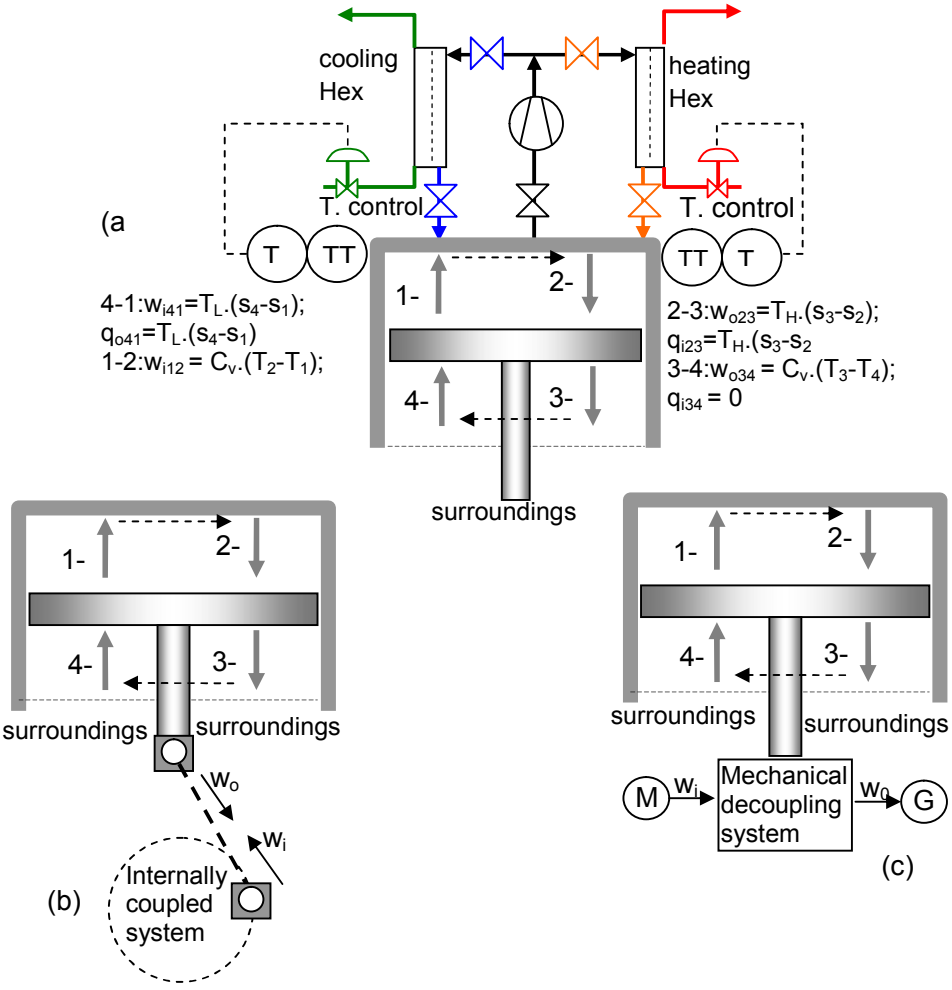

Fig. 4. Closed processes-based single-acting reciprocating engine structured to support a Carnot cycle and equipped with the cooling and heating temperature control devices necessary to implement isothermal processes: (a) General structure associated with forced convection heat (R. Ferreiro 2020 [20], Chapter 3,4,5) transfer devices, and temperature control; (b) internally coupled structure and (c) internally decoupled structure (by means of a hydraulic input-output work converter)

Downward stroke: Expansion Fig. 3 (a) and (b):

2-3 isothermal expansion with heat addition at T_H
3-4 adiabatic (isentropic) expansion.

Fig. 5 depicts the physical structure of a reversible open processes-based Carnot engine. This structure is intended for implementation in an open processes-based Carnot cycle. This plant represents a closed-circuit gas turbine composed of open processes.

The energy input-output energy balance for the plant structures depicted in Fig.5 is represented in Fig.6.

3.2 Analysis of a Carnot Cycle Considering Both Performance Criteria

3.2.1 Thermal efficiency

Carnot cycle transformations

With reference to Fig. 3 and Fig. 4, the transformations carried out along the compression and the expansion strokes composed by reversible closed processes include isothermal compression process 4-1, adiabatic compression 1.2, isothermal expansion 2-3, and adiabatic expansion 3-4, (modelled by the below equations).

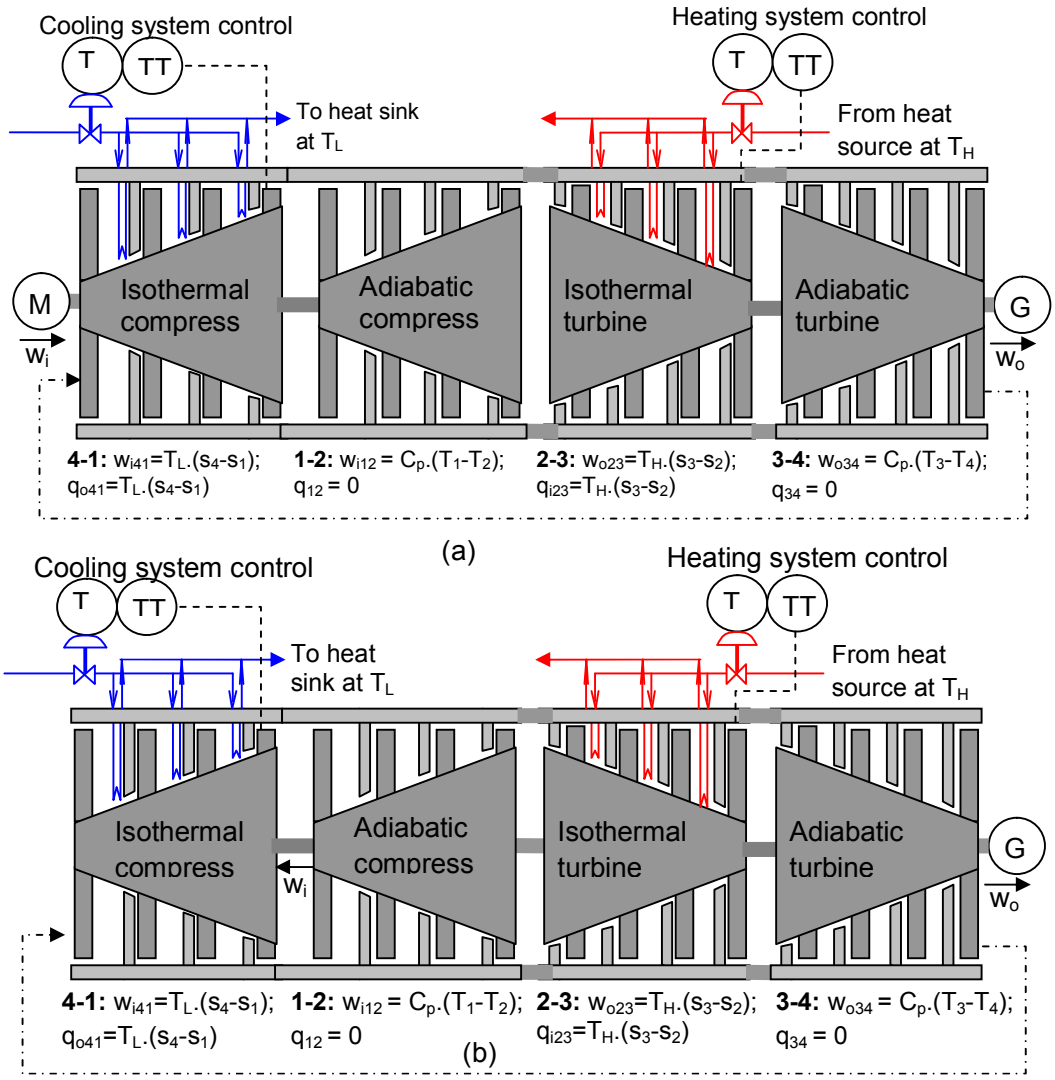

Fig. 5. Open processes-based rotary closed-circuit thermal engine structured to support a Carnot cycle, equipped with the cooling and heating temperature control devices necessary to implement isothermal processes: (a) internally decoupled and (b) internally coupled.

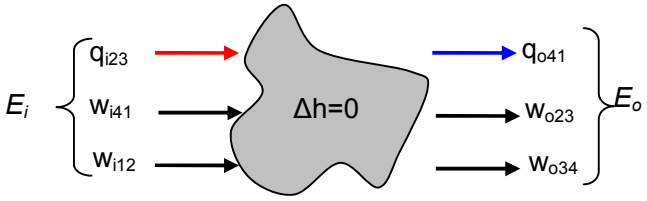

Fig. 6. The energy balance of the ideal Carnot cycle (losses are neglected).

Isothermal compression work

$$w_{i41} = T_1 \cdot (s_1 - s_4) \tag{23}$$

The isothermal compression work requires heat to be extracted along process 4-1 to keep the temperature constant at T_1

$$q_{o41} = T_1 \cdot (s_1 - s_4) \tag{24}$$

Adiabatic compression work along process 1-2

$$w_{i12} = Cv \cdot (T_2 - T_1) \tag{25}$$

Isothermal expansion work

$$w_{o23} = T_2 \cdot (s_3 - s_2) \tag{26}$$

The isothermal expansion work requires heat to be added along process 2-3 to keep the temperature constant at T_2

$$q_{i23} = T_1 \cdot (s_3 - s_2) \tag{27}$$

Adiabatic expansion work along process 3-4

$$w_{o34} = Cv \cdot (T_3 - T_4) = Cv \cdot (T_2 - T_1) \tag{28}$$

3.2.2 Cycle analysis

Based on Fig. 6, the cycle analysis is carried out as follows.

Input heat

$$q_{i23} = T_2 \cdot (s_3 - s_2) \tag{29}$$

Output heat

$$q_{o41} = T_1 \cdot (s_4 - s_1) \tag{30}$$

Net cycle heat and work

$$\begin{aligned} w_n &= q_i - q_o = q_{i23} - q_{o41} = \\ &= T_2 \cdot (s_3 - s_2) - T_1 \cdot (s_4 - s_1) = \\ &= \Delta s \cdot (T_2 - T_1) = \Delta s \cdot (T_H - T_L) \end{aligned} \tag{31}$$

Input work

$$\begin{aligned} w_i &= w_{i41} + w_{i12} \\ &= T_1 \cdot (s_4 - s_1) + Cv \cdot (T_2 - T_1) \end{aligned} \tag{32}$$

Output work

$$\begin{aligned} w_o &= w_{o23} + w_{o34} \\ &= T_2 \cdot (s_3 - s_2) + Cv \cdot (T_3 - T_4) \end{aligned} \tag{33}$$

For open processes (according to Figs. 5 and 6),

$$w_i = w_{i41} + w_{i12} = T_1 \cdot (s_4 - s_1) + Cp \cdot (T_2 - T_1) \tag{34}$$

$$w_o = w_{o23} + w_{o34} = T_2 \cdot (s_3 - s_2) + Cp \cdot (T_3 - T_4) \tag{35}$$

Net cycle work

$$\begin{aligned} w_n &= w_o - w_i = [T_2 \cdot (s_3 - s_2) + Cv \cdot (T_3 - T_4)] \\ &- [T_1 \cdot (s_4 - s_1) + Cv \cdot (T_2 - T_1)] = \\ &= \Delta s \cdot (T_2 - T_1) = \Delta s \cdot (T_H - T_L) \end{aligned} \tag{36}$$

As expected, Eq. (31) = Eq. (36). These results are based on the fact that

$$Cv \cdot (T_3 - T_4) = Cv \cdot (T_2 - T_1), \text{ and } (s_3 - s_2) = (s_4 - s_1) \tag{37}$$

3.2.3 Carnot cycle performance

According to the first law (represented in Fig. 6), the change in internal energy for a cycle is zero. Thus, for a reversible cycle (i.e. a cycle for which all losses are neglected), the balance between heat and work satisfies the following condition:

$$q_i + w_i - q_o - w_o = \Delta u = 0 \quad ;$$
$$q_i + w_i = q_o + w_o \tag{38}$$

The net work, from (31) and (34), is

$$q_i - q_o = w_o - w_i = w_n \tag{39}$$

3.2.3.1 Thermal efficiency

The thermal efficiency for closed processes—which, in this case, coincides with the thermal efficiency of a Carnot cycle or Carnot factor—is

$$\eta_{th} = \eta_C = \frac{w_n}{q_i} = \frac{\Delta s \cdot (T_2 - T_1)}{T_2 \cdot \Delta s} = 1 - \frac{T_1}{T_2} \tag{40}$$

Thus, the Carnot theorem is validated through the formulation of (38), which is supported by Eqs. (29)-(39).

3.2.3.1 Energetic efficiency

Since losses have been neglected, all inlet variables (heat and work) depicted in Fig. 6 represent a cost, which is assumed as an economic effort. Meanwhile, all outlet variables depicted in Fig. 6 represent the work done and rejected heat. According to a second law statement (Kelvin-Planck), the rejected heat cannot reach zero, although this condition is desirable. This means that the more useful work there is in the output energy factor, the lower the rejected heat and vice versa. So, under the given conditions, the goal is to reject the lowest amount of energy possible to maximise the benefits of the net work. Thus, according to the first law for the Carnot engine cycle (see Fig. 5) for which an internally decoupled engine is considered, it follows from Eq. (3) that

$$E_i - E_o = \sum q_i - \sum q_o + \sum w_i - \sum w_o = \Delta u = 0 \tag{41}$$

Particularly for the Carnot cycle (according to Figs. 3-6), it follows that

$$E_i - E_o = q_{i23} + w_{i41} + w_{i12} - q_{o41} - w_{o23} - w_{o34} = 0 \tag{42}$$

where

$$\begin{aligned} E_i &= q_{i23} + w_{i41} + w_{i12} \\ &= T_2 \cdot (s_3 - s_2) + T_1 \cdot (s_4 - s_1) + Cv \cdot (T_2 - T_1) \end{aligned} \tag{43}$$

and

$$\begin{aligned} E_o &= q_{o41} + w_{o23} + w_{o34} \\ &= T_1 \cdot (s_4 - s_1) + T_2 \cdot (s_3 - s_2) + Cv \cdot (T_3 - T_4) \end{aligned} \tag{44}$$

Then, the energy effort in terms of cost E_i is

$$E_i = q_{i23} + w_{i41} + w_{i12} \tag{45}$$

and the output useful work w_n in a reversible case is

$$w_o = E_o - q_{o41} = w_{o23} + w_{o34} \tag{46}$$

The energetic efficiency η_E, then, is the ratio of output useful work w_n to the cost of added energy E_i, per Eq. (47) below.

$$\eta_E = \frac{\sum w_o}{E_i} = \frac{w_{o23} + w_{o34}}{q_{i23} + w_{i41} + w_{i12}} \tag{47}$$

Thus, using the Carnot cycle formulation of heat and work—considering the data from Eq. (7), Table 1, and Table 2(b), the energetic efficiency can be expressed as

$$\begin{aligned} \eta_E &= \frac{w_o}{E_i} = \frac{T_2 \cdot (s_3 - s_2) + Cv \cdot (T_3 - T_4)}{T_2 \cdot (s_3 - s_2) + T_1 \cdot (s_1 - s_4) + Cv \cdot (T_2 - T_1)} \\ &= \frac{T_2 \cdot \Delta s + \Delta u_{34}}{T_2 \cdot \Delta s + \Delta u_{21} + T_1 \cdot \Delta s} \end{aligned} \tag{48}$$

For the case of open processes (according to Figs. 5 and 6), where the Carnot engine is implemented under a compressor and turbine that are internally decoupled from each other, the energetic efficiency is

$$\begin{aligned} \eta_E &= \frac{w_o}{E_i} = \frac{T_2 \cdot (s_3 - s_2) + Cp \cdot (T_3 - T_4)}{T_2 \cdot (s_3 - s_2) + T_1 \cdot (s_1 - s_4) + Cp \cdot (T_2 - T_1)} \\ &= \frac{T_2 \cdot \Delta s + \Delta h_{34}}{T_2 \cdot \Delta s + \Delta h_{21} + T_1 \cdot \Delta s} \end{aligned} \tag{49}$$

Tables 1 and 2(b) show that the energetic efficiency is greater than thermal efficiency. In other words, the result of Eq. (40) is lower than the result of Eqs. (48 and (49), according to the proposed *theorem 1* and *corollary 1*, or

$$\frac{T_2 \cdot \Delta s + \Delta u_{34}}{T_2 \cdot \Delta s + \Delta u_{21} + T_1 \cdot \Delta s} \text{ or } \frac{T_2 \cdot \Delta s + \Delta h_{34}}{T_2 \cdot \Delta s + \Delta h_{21} + T_1 \cdot \Delta s} > 1 - \frac{T_1}{T_2} \tag{50}$$

This relevant result will be analysed in the next section through the study of cases on a Carnot-based machine.

4. CASE STUDY

This section concerns the validation study carried out on a viable real Carnot engine considering two significant performance indexes where both a Carnot engine operating with closed processes and one operating with open processes under a Carnot thermal cycle are considered. The study consists of a series of cases carried out on two real Carnot machine structures e operating with the Carnot cycle, where water, helium and dry air are considered as real working fluids. Such structures consist of the following:

- an engine structure based on a single-acting a reciprocating cylinder internally coupled (see Fig. 4)
- an engine structure based on an internally decoupled set of compressor-expander engines (see Fig. 5)

The obtained results are compared to determine the behaviour of a real Carnot machine operating in both physical structures under two different performance criteria.

4.1 Performance Results

The data corresponding to the cycle computations of the five cases considered in the case study are depicted in Tables A1, A3, and A5 of Appendix 1. The computations were made at different top temperatures, with water, helium, and air used as the real thermal working fluid [21].

State point variables corresponding to the values of temperature (K), pressure (bar), specific volume (m^3/kg), internal energy (kJ/kg), and entropy (kJ/kg.K) as a function of the top temperatures considered are also depicted in Tables A1, A3, and A5.

Performance results are achieved by processing the data in Tables A1, A3, and A5 (shown in Appendix 1) to achieve the results depicted in Tables A2, A4, and A6, where the top temperatures T_H (K), lowest temperatures T_L (K), added heat q_i (kJ/kg), rejected heat q_o (kJ/kg), and net work w_n (kJ/kg) are depicted. Graphical results are presented in Fig. A7 when water was used as the real working fluid. Similar results are presented in Fig. A9 (for helium as the real working fluid) and Fig. A11 (for dry air as the real working fluid). Furthermore, thermal efficiency η_{th}=eff (%) (which is the ratio of the net output work to the input heat) is depicted for the case where the Carnot cycle coincides with the Carnot factor CF (%), as well as the energetic efficiency η_E, (which is the ratio of the net output work to the input added energy and which includes added heat and added work). Graphical results are presented in Fig. A8 (for real water as the real thermal working fluid), Fig. A10 (for helium as the real thermal working fluid), and Fig. A12 (for dry air as the real thermal working fluid).

The top temperature in all studied cases is limited to 1000 (K). The low temperature limit is fixed at 300 (K) for the cases of helium and air as the working fluid, while this value is 460 (K) for the case of water as the working fluid.

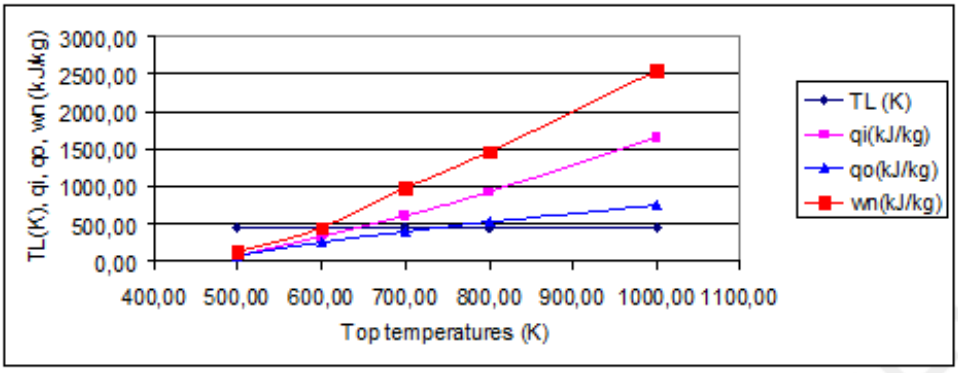

Fig. 7. Depiction of temperature (K), pressure (bar), specific volume (m^3/kg), internal energy (kJ/kg), and entropy (kJ/kg.K) as a function of the top temperatures for real water as the real working fluid (based on the data shown in Table A2)

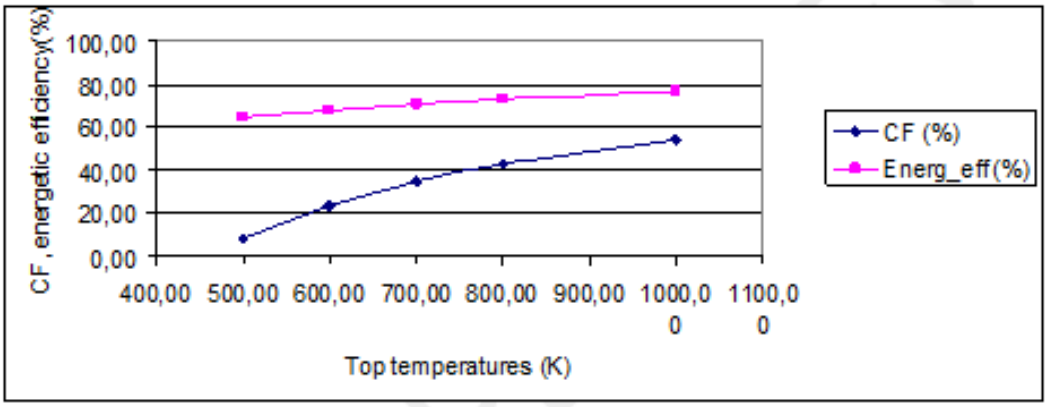

Fig. 8. Carnot factor, equivalent to the thermal efficiency η_{th} (%) and energetic efficiency η_E, for water as the real working fluid (based on the data shown in Table A2)

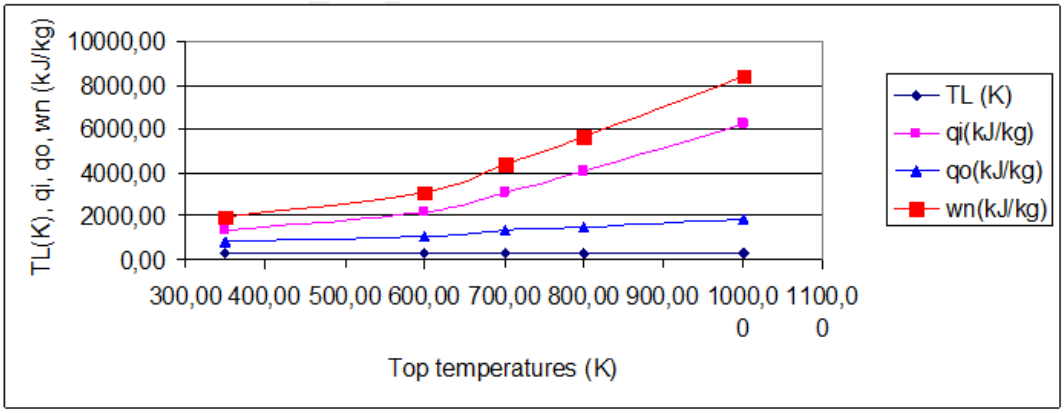

Fig. 9. Depiction of temperature (K), pressure (bar), specific volume (m^3/kg), internal energy (kJ/kg), and entropy (kJ/kg.K) as a function of the top temperatures for helium as the real working fluid (from the data shown in Table A4)

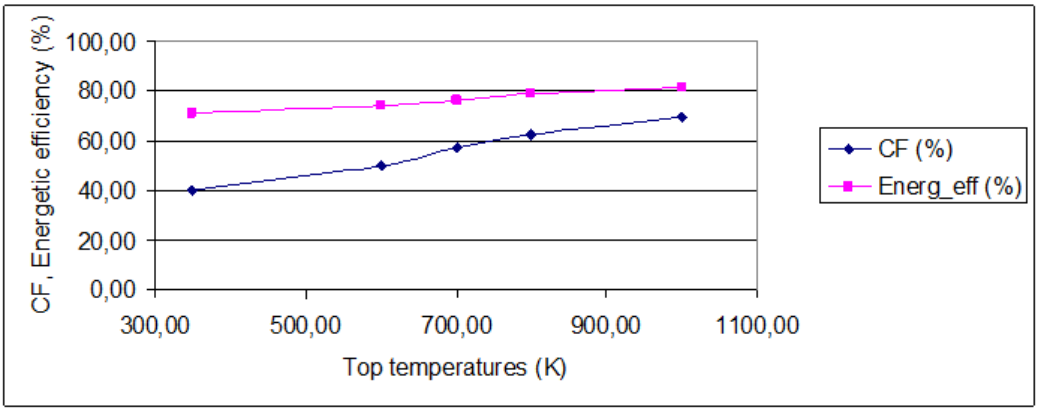

Fig. 10. Carnot factor, equivalent to the thermal efficiency η_{th} (%) and energetic efficiency η_E, for water as the real working fluid (based on the data shown in Table A4)

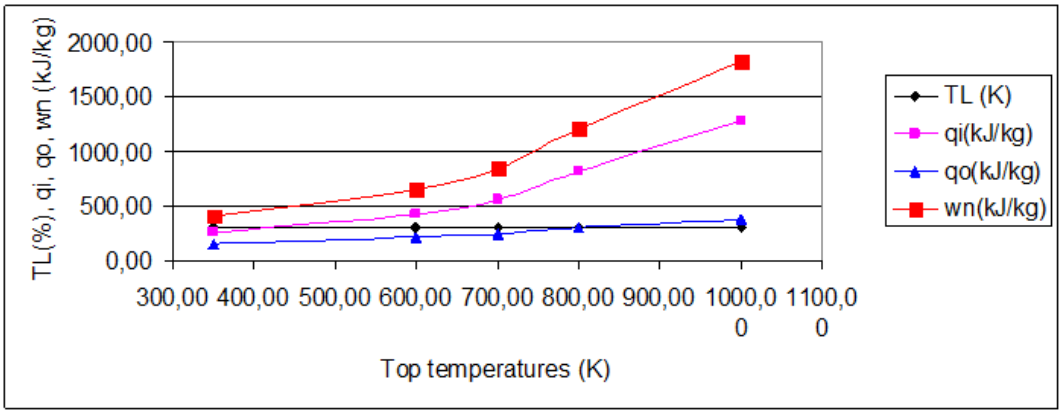

Fig. 11. Depiction of temperature (K), pressure (bar), specific volume (m^3/kg), internal energy (kJ/kg), and entropy (kJ/kg.K) as a function of the top temperatures for dry air as the real working fluid (based on the data shown in Table A6).

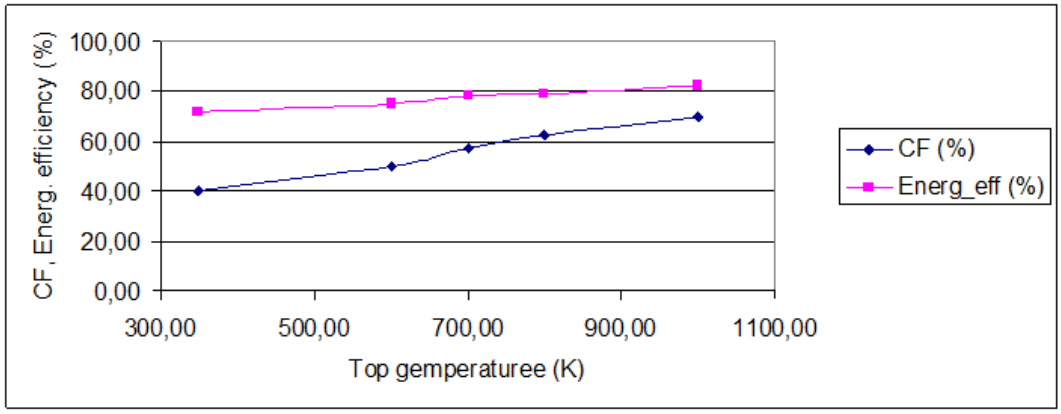

Fig. 12. Carnot factor, equivalent to the thermal efficiency η_{th} = eff (%) and energetic efficiency η_E, for water as the real working fluid (based on the data shown in Table A6)

5. DISCUSSION OF RESULTS

In the previous section, five cases were studied for each thermal working fluid (water, helium, and air). The results of the resolution of mentioned cases are represented in Appendix A (Tables A1, A3 and A5). The data shown in these tables have been analysed. The results of this analysis are depicted in Tables A2, A4, and A6.

From the observation of Tables A1, A3 and A5, it can be deduced that the specific works are medium for water, high for helium, and low for air. Thermal efficiencies (i.e. the ratio of net work to added heat) obviously correspond to the Carnot factor, and therefore, they turn out to be the same at the same temperature. Also, in internally coupled structures, the thermal efficiency turns out to be equal to the energy efficiency.

Regarding the internally decoupled structures (see Figures 8, 10, and 12), the energetic efficiencies (i.e. the ratio of net work to energy added, including any heat and work added to the cycle) differ substantially from the Carnot factor, which is widely surpassed for all thermal working fluids. It should be noted that the lower the limit temperature, the greater the difference between energy efficiency and thermal efficiency or Carnot factor.

In summary, as observed in all studied and analysed cases, thermal efficiency differs from energetic efficiency for all internal decoupled engines. For internally coupled engines, including Carnot-like engines, thermal efficiency

is identical to the energetic efficiency. However, for internally decoupled engines, thermal efficiency is significantly lower than energetic efficiency.

6. CONCLUSION

A preliminary study has been carried out on two Carnot-like machines structures. The proposed Carnot engine structures deal with reciprocating single- and double-acting cylinder-based thermal engines implemented under a Carnot cycle that is characterised by its mechanical structure and has been designed with mechanical internally coupled and decoupled structures.

Throughout this research, it has been shown that when using performance criteria based on first law efficiency—consisting of the ratio of net work to the added energy—it follows that, for reciprocating single and double-acting cylinders, forced convection-based isothermal heat transfer is feasible and effective. As such, a Carnot engine can be implemented if the engine speed is adapted to the heat transfer rate capacities.

A theorem and corollary for validating the performance of the Carnot engine based on internal decoupled structures demonstrated that the proposed Carnot engine is feasible and efficient in terms of energetic efficiency. It surpasses the thermal efficiency or Carnot factor for any operating condition within a specific range of operating temperatures. This characteristic assures us that a real Carnot machine is possible and efficient.

The results obtained through the resolution of some studied cases (according to Tables A3, A5 and A7) showed that a decoupled reversible Carnot engine structure operating with real working fluids surpasses the Carnot factor under all operating conditions. Furthermore, for low top temperatures, the difference between energetic and thermal efficiency is even greater.

This characteristic is interesting since the Carnot factor for low top temperatures is very low. Thus, this defect can be overcome in cases where the heat source provides low temperatures, thereby obtaining high performance with an internally decoupled Carnot engine structure.

COMPETING INTERESTS

Author has declared that no competing interests exist.

REFERENCES

1. Carnot S. “Reflexions sur la Puissance Motrice du Feu et sur les Machines” Propress a developer cette puissance. A Paris. Chez bachelier, Libraire, Quai ded Agustins. 1824;55.
   Available:https://gallica.bnf.fr/ark:/12148/bpt6k1170344j/f27.item
2. Moukalled F, Nuwayhid RY. The efficiency at maximum power output of a carnot engine with heat leak. International Journal of Mechanical Engineering Education. 1995;23(2):157-165.
   DOI:https://doi.org/10.1177/030641909502300210.
3. Bojić M. Cogeneration of power and heat by using endoreversible Carnot engine. Energy Conversion and Management. 1997;38(18):1877-1880.
   Available:https://doi.org/10.1016/S0196-8904(96)00110-0.
4. Stanislaw Sieniutycz. Generalized carnot problem of maximum work in finite time via Hamilton–Jacobi–Bellman theory, Energy Conversion and Management. 1998;1735-1743.
   DOI:https://doi.org/10.1016/S0196-8904(98)00084-3.
5. Ali Kodal, Bahri Sahin, Tamer Yilmaz. A comparative performance analysis of irreversible Carnot heat engines under maximum power density and maximum power conditions. Energy Conversion and Management. 2000;41(3):235-248.
   DOI: https://doi.org/10.1016/S0196-8904(99)00107-7.
6. Francesco di Liberto. Complexity in the stepwise ideal gas carnot cycle. Physica A: Statistical Mechanics and its Applications, 2002;314(1-4):331-344.
   DOI: https://doi.org/10.1016/S0378-4371(02) 01156-1.
7. Sánchez Salas N, Velasco S, Calvo Hernández A. Unified working regime of irreversible Carnot-like heat engines with nonlinear heat transfer laws. Energy Conversion and Management. 2002;43(17):2341-2348.
   DOI: https://doi.org/10.1016/S0196-8904(01)00169-8.
8. Tyagi SK, Kaushik SC, Singhal MK. Parametric study of irreversible Stirling and Ericsson cryogenic refrigeration cycles. Energy Conversion and Management. 2002;43(17):2297-2309.

DOI: https://doi.org/10.1016/S0196-8904(01)00181-9.

9. Lingen Chen, Xiaoqin Zhu, Fengrui Sun, Chih Wu. Optimal configuration and performance for a generalized Carnot cycle assuming the heat-transfer law $Q \propto (\Delta T)^m$ Applied Energy. 2004;78(3):305-313.
DOI:https://doi.org/10.1016/j.apenergy.2003.08.006.
10. M. Feidt, M. Costea, C. Petre, S. Petrescu, Optimization of the direct Carnot cycle, Applied Thermal Engineering, 2007. 27, (5–6),
DOI:https://doi.org/10.1016/j.applthermaleng.2006.09.020.
11. Jonathan M. Cullen, Julian M. Allwood. Theoretical efficiency limits for energy conversion devices, Energy. 2010;2059-2069.
DOI:
https://doi.org/10.1016/j.energy.2010.01.024.
12. Hamza Semmari, Driss Stitou, Sylvain Mauran. A novel Carnot-based cycle for ocean thermal energy conversion. Energy. 2012;43(1):361-375.
DOI:https://doi.org/10.1016/j.energy.2012.04.017;
13. Bing Zhou, XueTao Cheng, XinGang Liang Power and heat-work conversion efficiency analyses for the irreversible Carnot engines by entransy and entropy. Journal of Applied Physics. 2013;113;124904
DOI: https://doi.org/10.1063/1.4797494;
14. Blaise M, Feidt M, Maillet D. Optimization of the Changing Phase Fluid in a Carnot Type Engine for the Recovery of a Given Waste Heat Source. Entropy. 2015; 17(8):5503-5521.
DOI: https://doi.org/10.3390/e17085503;
15. Martínez I, Roldán É, Dinis L, et al. Brownian Carnot engine. Nature Phys. 2016;12:67-70.
DOI: https://doi.org/10.1038/nphys3518.
16. Michel Feidt. From carnot cycle to carnot heat engine: A case study. Finite Physical Dimensions Optimal Thermodynamics 1. Editor(s): Michel Feidt, Elsevier. 2017;75-97.
DOI:https://doi.org/10.1016/B978-1-78548-232-8.50003-0.
17. Mathilde Blaise, Michel Feidt, Denis Maillet. Influence of the working fluid properties on optimized power of an irreversible finite dimensions Carnot engine. Energy Conversion and Management. 2018;163:444-456.
DOI:https://doi.org/10.1016/j.enconman.2018.02.056.
18. Fontaine K, Yasunaga T, Ikegami Y. OTEC maximum net power output using carnot cycle and application to simplify heat exchanger selection. Entropy. 2019; 21(12):1143.
DOI:https://doi.org/10.3390/e21121143
19. Michel Feidt, Monica Costea. Progress in carnot and chambadal modeling of thermomechanical engine by considering entropy production and heat transfer entropy. Entropy. 2019;21:1232. DOI:10.3390/e21121232;
20. Ramon Ferreiro Garcia, Power Plants, Cycles: Advances and trends, Publisher: Book Publisher International, India, Published: Dec 12; 2020,
DOI: 10.9734/bpi/mono/978-93-90431-59-5; ISBN 978-93-90431-59-5 (Print), ISBN 978-93-90431-67-0 (eBook)
Available:http://www.bookpi.org/bookstore/product/power-plants-and-cycles-advances-and-trends/ .
21. Lemmon EW, Huber ML, McLinden MO. NIST reference fluid thermodynamic and transport Properties - REFPROP Version 8.0, User's Guide, NIST 2007, Boulder, Colorado.
Available:https://www.nist.gov/programs-projects/reference-fluid-thermodynamic-and-transport-properties-database-refprop;

APPENDIX

Table A1. Carnot cycle data tables for H2O

sp	T(K)	p(bar)	V(m^3/kg)	u(kJ/kg)	s(kJ/kg-K)
Case 1					
1	460.00	4.0000	0.51800	2626.00	7.1129
2	500.00	5.7018	0.39491	2684.60	7.1129
3	500.00	4.0000	0.56721	2689.90	7.2871
4	460.00	2.8093	0.74313	2631.10	7.2871
Case 2					
1	460.00	4.0000	0.51800	2626.00	7.1129
2	600.00	12.4840	0.21608	2833.50	7.1129
3	600.00	4.0000	0.68667	2847.60	7.6618
4	460.00	1.2847	1.64010	2637.30	7.6618
Case 3					
1	460.00	4.0000	0.51800	2626.00	7.1129
2	700.00	24.58	0.12777	2986.70	7.1129
3	700.00	4.00	0.80405	3008.60	7.9822
4	460.00	0.64931	3.25740	2639.80	7.9822
Case 4					
1	460.00	4.0000	0.51800	2626.00	7.1129
2	800.00	44.84	0.07986	3144.40	7.1129
3	800.00	4.00	0.92060	3175.10	8.2668
4	460.00	0.35237	6.01260	2640.90	8.2668
Case 5					
1	460.00	4.0000	0.51800	2626.00	7.1129
2	1000.00	127.0800	0.03513	3473.70	7.1129
3	1000.00	4.0000	1.15260	3528.00	8.7634
4	460.00	0.1207	17.58400	2641.80	8.7634

Table A2. Results of the analysis of the Carnot cycle from data tables for water as working fluid

TWF:H2O	Case 1	Case 2	Case 3	Case 4	Case 5
T_H (K)	500.00	600.00	700.00	800.00	1000.00
T_L (K)	460.00	460.00	460.00	460.00	460.00
q_i(kJ/kg)	87.10	329.24	608.51	923.12	1650.50
q_o(kJ/kg)	80.13	252.49	400.00	530.80	759.23
w_n(kJ/kg)	138.73	460.00	977.58	1457.32	2536.70
η_{th}=CF (%)	8.00	23.33	34.29	42.50	54.00
η_E=eff (%)	64.52	68.01	70.79	73.10	76.69

Table A3. Carnot cycle data tables for He

sp	T(K)	p(bar)	V(m^3/kg)	u(kJ/kg)	s(kJ/kg-K)
Case 1					
1	300.00	10.00	0.62613	940.13	23.2250
2	500.00	35.91	0.29200	1564.70	23.2250
3	500.00	10.00	1.04140	1563.50	25.8780
4	300.00	2.7878	2.23840	939.97	25.8780
Case 2					
1	300.00	10.00	0.62613	940.13	23.2250
2	600.00	56.68	0.22255	1877.40	23.2250

sp	T(K)	p(bar)	V(m^3/kg)	u(kJ/kg)	s(kJ/kg-K)
3	600.00	10.00	1.24900	1875.10	26.8250
4	300.00	1.767	3.52970	939.87	26.8250
Case 3					
1	300.00	10.00	0.62613	940.13	23.2250
2	700.00	83.39	0.17695	2190.50	23.2250
3	700.00	10.00	1.45670	2186.70	27.6250
4	300.00	1.2022	5.18660	939.86	27.6250
Case 4					
1	300.00	10.00	0.62613	940.13	23.2250
2	800.00	116.52	0.14512	2594.00	23.2250
3	800.00	10.00	1.66430	2498.30	28.3190
4	300.00	0.86074	7.24300	939.84	28.3190
Case 5					
1	300.00	10.00	0.62613	940.13	23.2250
2	1000.00	203.87	0.10426	3132.20	23.2250
3	1000.00	10.00	2.07970	3121.50	29.4770
4	300.00	0.4929	12.64600	939.83	29.4770

Table A4. Results of the analysis of the Carnot cycle from data tables for helium as working fluid

TWF:He	Case 1	Case 2	Case 3	Case 4	Case 5
T_H (K)	500.00	600.00	700.00	800.00	1000.00
T_L (K)	300.00	300.00	300.00	300.00	300.00
q_i(kJ/kg)	1326.50	2160.00	3080.00	4075.20	6252.00
q_o(kJ/kg)	795.90	1080.00	1320.00	1528.20	1875.60
w_n(kJ/kg)	1950.03	3095.23	4326.84	5633.66	8433.67
η_{th}=CF (%)	40.00	50.00	57.14	62.50	70.00
η_E=eff (%)	71.03	74.15	76.64	78.94	81.83

Table A5. Carnot cycle data tables for Air

sp	T(K)	p(bar)	V(m^3/kg)	u(kJ/kg)	s(kJ/kg-K)
Case 1					
1	300.00	10.00	0.08587	338.41	3.2236
2	500.00	59.76	0.02454	480.18	3.2236
3	500.00	10.00	0.14400	484.94	3.7460
4	300.00	1.6517	0.52110	340.08	3.7460
Case 2					
1	300.00	10.00	0.08587	338.41	3.2236
2	600.00	114.87	0.01569	552.95	3.2236
3	600.00	10.00	0.17286	560.44	3.9362
4	300.00	0.85304	1.00920	340.24	3.9362
Case 3					
1	300.00	10.00	0.08587	338.41	3.2236
2	700.00	202.04	0.01075	637.70	3.2236
3	700.00	10.00	0.20167	638.17	4.0100
4	300.00	0.65994	1.30460	340.28	4.0100
Case 4					
1	300.00	10.00	0.08587	338.41	3.2236
2	800.00	333.36	0.00778	704.68	3.2236
3	800.00	10.00	0.23044	718.25	4.2457
4	300.00	0.29632	2.96320	340.35	4.2457
Case 5					
1	300.00	10.00	0.08587	338.41	3.2236
2	1000.00	791.77	0.00460	865.79	3.2236

sp	T(K)	p(bar)	V(m^3/kg)	u(kJ/kg)	s(kJ/kg-K)
3	1000.00	10.00	0.28794	885.08	4.4958
4	300.00	0.12163	7.07960	330.37	4.4958

Table A6. Results of the analysis of the Carnot cycle from data tables for dry air as working fluid

TWF:AIR	Case 1	Case 2	Case 3	Case 4	Case 5
T_H (K)	350.00	600.00	700.00	800.00	1000.00
T_L (K)	300.00	300.00	300.00	300.00	300.00
q_i(kJ/kg)	261.20	427.56	550.51	817.68	1272.20
q_o(kJ/kg)	156.72	213.78	235.93	306.63	381.66
w_n(kJ/kg)	406.06	647.80	848.40	1195.58	1826.91
η_{th}=CF (%)	40.00	50.00	57.14	62.50	70.00
η_E=eff (%)	72.00	75.02	78.27	79.27	82.50

Peer-review history:
The peer review history for this paper can be accessed here:
http://www.sdiarticle4.com/review-history/67379